Sentinel Lymph Node Localization in Early Breast Cancer

Seza A. Gulec, Frederick L. Moffat, Robert G. Carroll, Aldo N. Serafini, George N. Sfakianakis, Lisa Allen, Jodeen Boggs, Dora Escobedo, Christopher S. Pruett, Anurag Gupta, Alan S. Livingstone and David N. Krag

Divisions of Nuclear Medicine and Surgical Oncology, Sylvester Comprehensive Cancer Center, University of Miami School of Medicine and Jackson Memorial Medical Center, Miami, Florida; Nuclear Medicine Department, Bay Pines VA Medical Center, Bay Pines, Florida; and Division of Surgical Oncology, University of Vermont Medical Center, Burlington, Vermont

Methods: Thirty-two patients with clinical node-negative breast cancer underwent sentinel node localization study as part of a National Cancer Institute-sponsored multicenter trial. Anatomical and histopathologic characteristics of sentinel lymph node (SLN) and a kinetic analysis of nodal uptake were studied. Patients were injected with 1 mCi/4 ml unfiltered ^{99m}Tc-sulfur colloid in four divided doses around the palpable lesion or immediately adjacent to the excision cavity if prior biopsy was performed. SLN biopsy was performed 1.5–6 hr (mean = 3 hr) postinjection. Intraoperative localization was performed using a gamma probe. All patients underwent complete axillary dissection. **Results:** SLN was identified in 30 of 32 (94%) patients. There were no false-negative SLN biopsies. **Conclusion:** This study supports the clinical validity of SLN biopsy in breast cancer and confirms that, unlike the blue dye technique, the learning curve with unfiltered ^{99m}Tc-sulfur colloid and the gamma detection probe is short, and SLN localization is achievable in over 90% of cases by surgeons with modest experience. The use of unfiltered ^{99m}Tc-sulfur colloid (larger particle size) with larger injected volume permits effective localization of SLNs.

Key Words: breast cancer; sentinel node; sulfur colloid; intraoperative gamma probe

J Nucl Med 1998; 39:1388–1393

The sentinel lymph node (SLN) is that lymph node (LN) in a given lymphatic basin that is first in line to receive lymphatic flow from a primary tumor site; this node should, therefore, be the first to become involved by metastasis from the tumor. The histological status of the SLN thus should be highly predictive of metastatic involvement of the LN basin in which it is situated.

Lymphangiographically directed SLN biopsy (SLNB) for penile carcinoma was described by Cabanas (*1*). SLNB using intradermal vital blue dye injections has been developed by Morton et al. (*2*) as a means of triage of patients with clinical node-negative (cN−) malignant melanoma for therapeutic regional lymphadenectomy. Alex et al. (*3,4*) and Krag et al. (*5,6*) reported a modification of this technique, in which ^{99m}Tc-sulfur colloid and a gamma detection probe (GDP) were used in lieu of blue dye. There are ample published data supporting the concept that the histological status of the SLN in melanoma patients reflects that of the remainder of the basin (*3–10*). Experience with these techniques changed the routine use of elective LN dissection in patients with intermediate-thickness lesions, and SLNB has become a standard of care in the management of cN–melanoma.

Routine axillary node dissection (AND) is currently the standard of care in cN− breast cancer. The pathological status of regional LNs has very significant prognostic and adjuvant therapeutic implications. However, 70%–80% of cN− breast cancer patients prove to be pathologically node negative. Although AND is, therefore, unnecessary in these patients in retrospect, they nonetheless must sustain the expense and potential morbidity of this procedure. Upper-extremity lymphoedema can be anticipated in 5%–8% of breast cancer patients undergoing AND (*11,12*).

It has traditionally been thought that metastasizing breast cancer cells spread in an orderly manner from the breast to the lower axillary nodes (Berg's level I) and from there to levels II and III. However, in 1.5%–14% of patients, "skip" metastases have been found in the higher levels in the absence of involvement of level I nodes (*13–18*). These metastasizing cells were presumed to have passed through level I and seeded out in the more distal nodes. Experience with lymphoscintigraphy and SLNB strongly suggests that these are SLNs and not skip metastases.

Unusual distributions of axillary metastases in breast cancer are explainable by variations in lymphatic anatomy and flow patterns with sentinel nodes being located in level II, level III, interpectoral, internal mammary, intramammary or supraclavicular areas in some patients. Different parts of the breast drain to different parts of the axilla and other first-order nodal basins; SLN location can, therefore, be expected to vary from one individual to another.

Of the various strategies explored to date in an effort to avoid unnecessary AND in cN− breast cancer, SLNB shows the most promise. Early reports using the blue dye method (*19,20*), blue dye with radiocolloid/GDP (*21*) or radiocolloids and an operative GDP (*4*) suggest that the probability of the SLN being negative for tumor when, in fact, metastases are present in the regional nodes (false-negative SLNB) in breast cancer is less than 2%.

McCarthy et al. (*22*) have averred that ^{99m}Tc-sulfur colloid should perform poorly in SLNB, basing this opinion on their observation with ^{99m}Tc-antimony sulfur colloid that pass-through of radioactivity to non-SLNs is time dependent and rapid. Technetium-99m-antimony sulfur colloid is an excellent radiocolloid for external lymphoscintigraphy and mapping of lymphatic basins because of its rapid migration through LNs; this trait is due to the small mean particle size (15 nm) of this radiocolloid. However, the ideal radiocolloid for SLNB should migrate in a reasonable time frame (0.5–1 hr) in sufficient quantities to be detectable with a GDP. Moreover, radiocolloid retention in SLNs and delay of pass-through to non-SLNs should be sufficiently long to permit SLNB to be performed over a wide range of time intervals (0.5–8 hr) after injection of the colloid. This degree of latitude would obviate potential

Received Jun. 26, 1997; revision accepted Nov. 24, 1997.

For correspondence or reprints contact: Frederick L. Moffat, MD, Sylvester Comprehensive Cancer Center, 1475 NW 12th Ave., Miami, FL 33136.

logistical problems in surgical scheduling. Because the rate of radiocolloid migration through lymphatics and nodal basins is inversely proportional to radioparticle size (*23*), unfiltered ^{99m}Tc-sulfur colloid could be better suited for SLNB than smaller colloids. In practice, this radiocolloid appears to be quite suitable for this application (*3,4,6,21,23*).

SLNB using unfiltered ^{99m}Tc-sulfur colloid and a GDP is being evaluated in an National Cancer Institute-sponsored multicenter trial. We report an analysis of the kinetics of unfiltered ^{99m}Tc-sulfur colloid in this SLNB protocol in cN− breast cancer patients.

MATERIALS AND METHODS

Patients and Study Protocol

This analysis was performed on the first 32 patients (age range 25–65 yr) accrued at the University of Miami/Jackson Memorial Medical Center to a National Cancer Institute-sponsored prospective multicenter trial of SLNB in breast cancer. Eligibility criteria specified patients with unifocal primary invasive breast cancer scheduled for mastectomy/lumpectomy and axillary LN dissection, minimum age of 18 yr and Karnofsky performance status of 70 or greater. Patients with multicentric primary breast cancer, noninvasive breast cancer or clinically positive regional LNs were excluded. The protocol was approved by the University of Miami institutional review board, and prior written informed consent was obtained from all patients.

Radiopharmaceutical and Injection Technique

Unfiltered ^{99m}Tc-sulfur colloid (Mallinckrodt, St. Louis, MO; 1 mCi in 4 ml normal saline) was injected in four divided doses (0.25 mCi in 1 ml) into the breast parenchyma around the palpable primary cancer or immediately adjacent to the excision cavity if prior biopsy had been performed. The injections were given superior, inferior, medial and lateral to the primary tumor site. A 1.5-inch, 25- or 27-gauge needle was used to deposit ^{99m}Tc-sulfur colloid around the primary tumor site and to prevent backflow of the radiocolloid through the needle puncture wound.

Gamma Detection Probe

Intraoperative localization was performed using a GDP (C-TRAK, Care Wise, Morgan Hill, CA). The 140-keV photopeak of ^{99m}Tc was captured with a 20% window riding on a threshold of 130 keV. The probe sensitivity was 800 counts/sec/μCi ^{99m}Tc at contact.

Intraoperative Lymphatic Mapping and Sentinel Lymph Node Biopsy

All operations were performed by one surgeon. The GDP probe was ensheathed in a sterile ultrasound probe cover, and a sterile glove was tied over the end of the probe as extra security against breaks in surgical technique. Vital blue dyes were not used in any of these patients.

After induction of general anesthesia, skin preparation and draping of the operative field, a 10-sec probe count was taken over the right lobe of the liver to document any systemic absorption of the radiocolloid. The perimeter of radioactivity at the ^{99m}Tc-sulfur colloid injection site was mapped with the GDP and marked on the breast skin. The breast was then scanned radially from the nipple in all directions with the GDP to seek out any intramammary radiolocalizations. The axillary, supraclavicular, infraclavicular, parasternal and rectus sheath regions were then surveyed with the GDP, moving the instrument methodically in a grid pattern over the skin. Cutaneous hot spots were delineated and carefully marked; these signify the accumulation of radioactivity in one or more underlying SLNs. A hot spot was defined as a focus of increased radioactivity with a 10-sec count of at least 25 and at least three times that of the adjacent normal skin. When there was more than one hot spot, these were identified by number (1, 2, 3, and so on) and location for subsequent analysis. Sentinel lymph node biopsy proceeded after all hot spots had been identified and counted. The duration of hot spot localization procedure was 10–15 min.

In patients undergoing total mastectomy (which by chance included the three patients who had internal mammary SLNs), mastectomy flaps developed and SLNB was performed through the mastectomy wound to spare the patient extra incisions. In all patients undergoing lumpectomy who had SLNs in the axilla only, SLNB was performed through a standard anteroposterior incision placed in the lower axillary hair-bearing skin, with development of superior and inferior skin flaps, as is routinely performed in formal axillary lymphadenectomy.

Dissection was directed entirely by the GDP, using sharp dissection in the direction of maximal radioactivity. The radioactive node(s) encountered was removed, and a 10-sec count of each node was obtained ex vivo, pointing the probe at the ceiling and placing the node on the probe. The location of each SLN (axillary levels I, II and III and internal mammary) was recorded.

When multiple radioactive nodes were found under a hot spot, only those with at least 10% of the ex vivo count of the hottest SLN were considered SLNs. All SLNs were measured in three dimensions and submitted to pathology in formalin, labeling each by hot spot number and ex vivo 10-sec count number for accurate identification during subsequent analysis. The SLNB wound was then resurveyed with the probe for residual radioactivity in the SLN bed; only when the SLN bed activity was less than 10% of the ex vivo count of the hottest SLN was the SLNB procedure deemed complete.

In patients with parasternal hot spots, the pectoralis muscle was split in the direction of its fibers over the point of maximum radioactivity. An underlying costochondral junction was encountered, and the maximal activity was always at the articulation of the superior border of the rib cartilage with the sternum. The intercostal muscles were dissected from the superior border of the rib cartilage, and the underlying mediastinum and pleural reflection were exposed. The internal mammary vessels were usually seen, and the internal mammary SLN was found just behind the superior border of the cartilage and the sternum.

Total axillary lymphadenectomy was performed as previously described (*25*); however, levels I, II and III were carefully delineated with sutures in situ, and tissues resected from each level were labeled and submitted as separate specimens for ease of identification during analysis. All resected axillary tissues were scanned with the probe ex vivo to detect any radioactive LNs that were not under hot spots (defined as nodes with a 10-sec ex vivo count of at least 10% of that of the hottest axillary SLN).

Pathologic Evaluation

Histopathologic analysis was performed by microscopic examination of one or two sections from each bivalved SLN and non-SLN.

Kinetic Measurements of Nodal Uptake

SLNs were carefully measured in three dimensions immediately after removal. Ex vivo volume and radioactivity measurements were obtained. Nodal activities were expressed as the percentage of injected dose per gram of tissue. Volume was measured using the formula $V = 4/3\pi r^3$, and conversion of volume to weight was performed using 1 ml = 1 g assumption. Count-activity conversion was based on the probe sensitivity of 800 counts/sec/μCi.

TABLE 1
Histopathologic Diagnosis, Primary Tumor Size and Location

Patient	Pathologic diagnosis	Primary size (cm)	Location
1	Infiltrating ductal	3.1	Lower central
2	Infiltrating ductal	1.5	Outer central
3	Infiltrating ductal	1.3	Upper central
4	Infiltrating Ca, solid	0.6	UOQ
5	Infiltrating ductal	1.5	UIQ
6	Infiltrating ductal	1	Upper central
7	Infiltrating ductal and lobular	0.7	Inner central
8	Infiltrating ductal	1.2	LOQ
9	Infiltrating ductal	0.5	UOQ
10	Infiltrating ductal	2	Upper central
11	Infiltrating ductal	3.2	Central
12	Infiltrating ductal	1.4	Central
13	Infiltrating ductal	0.9	Lower central
14	Infiltrating ductal	3	UOQ
15	Infiltrating ductal	1.3	UIQ
16	Infiltrating ductal	1.5	Central
17	Infiltrating ductal	2.5	UOQ
18	Infiltrating ductal	1.2	Upper central
19	Infiltrating ductal	3.5	UOQ
20	Infiltrating ductal	3.5	Upper central
21	Infiltrating ductal and DCIS	0.2	Central
22	Infiltrating ductal	1.5	UOQ
23	Infiltrating ductal	3.5	Central
24	Infiltrating ductal and in situ lobular	6	UOQ
25	Infiltrating ductal	0.9	Upper central
26	Infiltrating ductal	4	Upper central
27	Infiltrating ductal	2.1	UIQ
28	Infiltrating ductal	0.8	UIQ
29	Infiltrating ductal	0.5	Central
30	Infiltrating ductal and DCIS	3	UOQ
31	Infiltrating ductal	1.6	Upper central
32	Infiltrating ductal	2.7	UOQ

UOQ = upper outer quadrant; LOQ = lower outer quadrant; UIQ = upper inner quadrant; DCIS = ductal carcinoma in situ.

RESULTS

Primary Tumor Characteristics

Thirty-one patients had infiltrating ductal cancer. One patient had invasive colloid carcinoma. Primary tumor stage was T_1 in 20 patients, T_2 in 11 patients and T_3 in 1 patient. Details of primary tumor characteristics are given in Table 1.

Technical Success

One or more SLNs were identified in 30 of 32 (94%) patients.

Anatomical and Histopathologic Characteristics of Sentinel Lymph Nodes

The total number of nodes dissected and the total number of SLNs identified were 654 and 74, respectively. One SLN was identified in 11 of 30 (37%) patients, and multiple nodes were detected in 19 of 30 (63%) patients. Sixty of 74 (81%) SLNs were situated in axilla level I, 11 of 74 (15%) were situated in axilla level II and 3 of 74 (4%) were situated in internal mammary. There were no false-negative SLN biopsies. In 1 patient, a node with an activity of less than 10% that of the SLN (which was immediately adjacent to the SLN) was confirmed to contain metastasis. Histopathologic analysis of the node revealed near-complete replacement of normal LN structure with metastatic tumor (Fig. 1). Details of anatomical and histopathologic characteristics of SLNs are given in Table 2. Correlation matrix for the metastasis status of sentinel and nonsentinel LNs is given in Table 3.

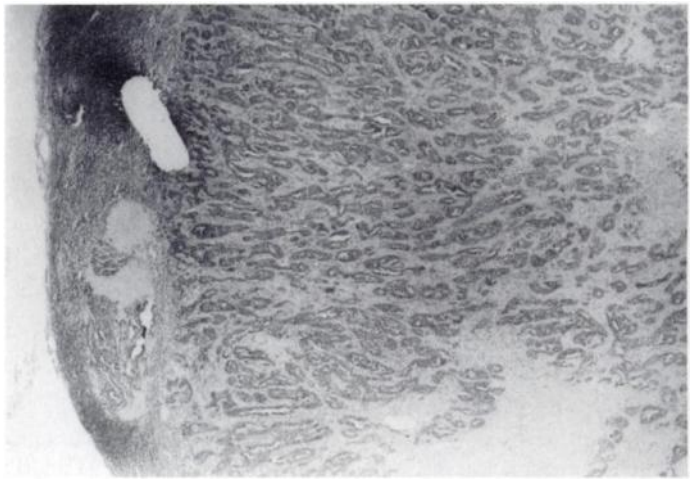

FIGURE 1. Histopathology of a nonsentinel lymph node (LN) in Patient 24. The two sentinel lymph nodes (SLNs) had 2039 and 349 counts. Both SLNs were histologically tumor free. This LN had 61 counts, disqualifying it to be considered as a SLN. Histopathology shows near-complete infiltration of the node, with tumor leaving only a narrow rim of normal lymphoid paranchyma to localize the radiocolloid.

Nodal Uptake Kinetics

These data are given in Table 4. SLN masses ranged from 0.01 to 11.5 g (mean = 1.2 g). Individual nodal uptake was between 0.0003 and 0.8 (mean = 0.05) of the percentage of injected dose per gram of tissue.

Toxicity and Adverse Effects

There were no allergic or idiosyncratic events related to the use of ^{99m}Tc-sulfur colloid. None of the patients had any wound complications. None of the patients who underwent internal mammary SLNB suffered any complications, such as internal mammary artery hemorrhage or pneumothorax.

DISCUSSION

The clinical applicability of SLNB in the patient depends primarily on the negative predictive value of SLN status. SLNB in cutaneous melanoma, with a 98% negative predictive value, is much preferred to therapeutic lymphadenectomy in cN− patients. The National Cancer Institute-sponsored multicenter trial will clarify the clinical applicability of the technique in breast cancer patients by establishing the negative predictive value of SLNB in a large number of patients. An interim analysis on the first 155 patients was very encouraging and revealed only two false-negative SLNBs (Krag DN, *personal communication*).

In malignant melanoma, the rich intradermal lymphatic network enables quick and effective localization of regional LN with small injected volumes of radiocolloid. In breast cancer, radiocolloid is injected into the breast tissue around the primary tumor or into the walls of the biopsy cavity. Because the lymphatics in breast parenchyma are sparse relative to those in the dermis, the dose and volume of injected radiotracer are more important factors in sentinel node localization in breast cancer. The technical challenges of SLN localization center around three issues:

1. The success rate of identifying a SLN;
2. Confinement of radiolabeling to the SLN(s) rather than more distal nodes; and
3. The surgical learning curve associated with SLNB.

The success rate of breast cancer SLN identification using radiocolloid and a GDP appears to be related to the injected volume. In preliminary studies, small injection volumes (<4

TABLE 2
Anatomical Distribution of Sentinel Lymph Nodes According to the Regional Nodal Basins: Metastatic Involvement in the Sentinel and Non-Sentinel Lymph Nodes

	Anatomical location						Metastatic status						
Patient	1	2	3	4	5	6	1	2	3	4	5	6	Remainder
1	AI						POS						1/28
2	X	X	X	X	X	X	X	X	X	X	X	X	0/38
3	AI	IM	AI				NEG	NEG	POS				0/36
4	AI						NEG						0/20
5	AI	AI	AI				NEG	POS	NEG				0/8
6	AI	AI	AII	AI	AII	IM	NEG	NEG	NEG	NEG	NEG	NEG	0/14
7	AI						NEG						0/15
8	AI						NEG						0/19
9	AI	AI	AI	AI	AI	AI	NEG	NEG	NEG	NEG	NEG	NEG	0/13
10	AI						NEG						0/32
11	AI						NEG						0/21
12	AI	AI	AI				NEG	NEG	NEG				0/27
13	AI	IM	AII	AI			NEG	NEG	NEG	NEG			0/15
14	AI						NEG						0/29
15	AI	AII	AI				NEG	NEG	NEG				0/22
16	AI						NEG						0/20
17	AI	AI					NEG	NEG					0/26
18	AI	AI	AI				NEG	NEG	NEG				0/21
19	AI						NEG						0/28
20	AI	AI	AI	AI			POS	POS	NEG	NEG			0/15
21	AI	AI	AII	AII	AII		NEG	NEG	NEG	NEG	NEG		0/12
22	AI	AI	AII				NEG	NEG	NEG				0/21
23	AI	AII					NEG	NEG					0/13
24	AI	AI	AI	AI			NEG	NEG	NEG	POS			16/27
25	AI						NEG						0/17
26	AI						NEG						0/16
27	X	X	X	X	X	X	X	X	X	X	X	X	0/32
28	AI	AII					NEG	NEG					0/14
29	AI	AI					POS	POS					0/16
30	AI	AI					POS	POS					3/8
31	AI	AI	AI				POS	POS	NEG				0/17
32	AI	AII					NEG	NEG					0/14

AI = axilla level I; AII = axilla level II; IM = internal mammary; NEG = negative for metastasis; POS = positive for metastasis; X = no sentinel lymph node identified.

ml) were associated with low localization rates (~70%) (*4*). In this study, using a ^{99m}Tc-sulfur colloid injection volume of 4 ml, there were two patients in whom a SLN could not be localized. In a recent pilot study in which ^{99m}Tc-sulfur colloid volume was increased to 8 ml, the radiolocalization rate was 100% (Krag DN, *personal communication*).

The volume dependency of SLN radiolabeling can be explained by the basic histologic and functional properties of lymphatics. Lymphatic capillaries are composed of endothelial cells that overlap each other to varying degrees. Unlike the vascular endothelium, the lymphatic endothelial cells do not rest on a continuous basal membrane. Instead, they are suspended within surrounding interstitial tissue by longitudinal bundles of collagen fibers called anchoring filaments. These anchoring filaments occur at regular intervals along the lymphatic vessel wall, and they are seen on surfaces of endothelial projections and the overlapping terminal margins of adjacent endothelial cells, the so-called patent junctions. An increase in fluid volume in interstitial tissues stretches the fibers, causing passive separation of adjacent endothelial cells and allowing more rapid intraluminal migration of the injected radiocolloid particles (*23*). On the other hand, injection of excessive volumes may lead to labeling of nodes that are not draining the tumor, and therefore, some of the identified SLNs may not be the actual SLNs. This theoretical consideration, however, might not be clinically relevant.

TABLE 3
Correlation Matrix for the Metastasis Status of Sentinel and Non-Sentinel Lymph Nodes

	nSLN(−)	nSLN(+)
SLN(−)	24	0 (1)
SLN(+)	3	4

A non-sentinel lymph node (nSLN) in Patient 24: low level of activity is due to near-complete infiltration of the node with tumor.

The number of radiolabeled LNs in a basin is related in part to the particle size of the injected radiocolloid. It has been shown that the optimal radiocolloid particle size is in the range of 5–15 nm for visualization of the maximum number of LNs in a given nodal basin (*24*). It has also been shown that lymphoscintigraphies performed with very large radioparticles, such as sulfur colloid, failed to visualize 50% of the normal nodes at a draining basin (*24*).

Strand and Persson (*24*) compared the kinetics of ^{99m}Tc-labeled sulfur colloid, tin colloid, antimony sulfur colloid, sodium tin phytate, ^{198}Au-colloid and ^{99m}Tc-human serum albumin in a rabbit model. The time-activity curve pattern for regional nodal uptake was similar for all radiocolloids tested.

TABLE 4
Masses and Activities of the Sentinel Lymph Nodes

	Mass (g)						Injected dose/g of tissue					
Patient	1	2	3	4	5	6	1	2	3	4	5	6
1	1.8						0.003					
2	X	X	X	X		X	X	X	X	X	X	X
3	0.5	0.07	0.07				0.06	0.06	0.01			
4	3						0.0006					
5	0.4	0.07	0.1				0.05	0.2	0.02			
6	1.4	0.4	0.5	0.7	0.1	0.01	0.02	0.06	0.03	0.01	0.06	0.8
7	1.2						0.004					
8	3.4						0.002					
9	0.5	0.3	1.8	1.8	0.2	0.4	0.04	0.04	0.006	0.004	0.03	0.01
10	0.01						0.2					
11	0.5						0.1					
12	1.4	0.3	0.5				0.006	0.01	0.002			
13	0.5	0.2	0.5	0.2			0.04	0.04	0.006	0.02		
14	0.2						0.1					
15	0.5	0.3	0.5				0.006	0.007	0.002			
16	0.5						0.006					
17	0.4	1.2					0.008	0.0008				
18	11.5	1.8	0.5				0.0004	0.0004	0.001			
19	3						0.007					
20	4	0.5	0.2	0.5			0.005	0.01	0.02	0.004		
21	0.3	0.5	1	1	0.3		0.1	0.02	0.009	0.003	0.01	
22	5	4	0.3				0.001	0.0003	0.003			
23	1.8	0.5					0.002	0.001				
24	0.9	0.07	0.9	0.5			0.1	0.3	0.02	0.001		
25	1.8						0.001					
26	4.2						0.01					
27	X	X	X	X	X	X	X	X	X	X	X	X
28	1.4	0.5					0.0007	0.2				
29	0.7	0.5					0.4	0.06				
30	1.4	0.5					0.2	0.1				
31	4.2	4.2	4.2				0.0005	0.0007	0.0005			
32	1.4	0.3					0.2	0.07				

Uptake in the LNs started immediately after the injection, and a plateau was reached after approximately 2 hr. The highest nodal uptake (9% of injected activity) was observed with ^{198}Au-colloid. This was followed by antimony sulfur colloid with about 5% nodal uptake. Sulfur colloid had the lowest nodal uptake values.

Technetium-99m-sulfur colloid is the only sulfur-based lymphoscintigraphy agent available in the U.S. The particle size of unfiltered sulfur colloid ranges from 50–1000 nm (average size = 200 nm). Sulfur colloid particles undergo conspicuous changes in diameter, both while standing in a closed vial and/or after injection into tissues. Solutions of smaller particle size comparable with ^{99m}Tc-antimony sulfur colloid can be obtained by different preparation techniques and filtration. A preparation technique and kinetic properties of filtered sulfur colloid were recently described by Hung et al. (*26*). The average particle size ranged between 15 and 50 nm. The average radioactivity retained in the filter was 62.7%–10.1% of the total activity. Nineteen patients studied with filtered sulfur colloid demonstrated lymphoscintigraphic patterns similar to those seen on ^{99m}Tc-antimony sulfur colloid images.

For complete mapping of a lymphatic basin, smaller-sized radiocolloids undoubtedly give better results (*27*). However, for SLN localization, it is desirable not to radiolabel the more distant LNs; therefore, unfiltered ^{99m}Tc-sulfur colloid might be preferable in this setting. This hypothetical deduction obviously remains to be proven with comparative studies.

CONCLUSION

This study supports the clinical validity of SLNB in breast cancer and confirms that, unlike the blue dye technique, the learning curve with unfiltered ^{99m}Tc-sulfur colloid and the GDP is short, and SLN localization is achievable in over 90% of cases by surgeons with modest experience. The use of unfiltered ^{99m}Tc-sulfur colloid (larger particle size) with larger injected volume permits effective localization of SLN(s). The theoretical problems posed by low levels of lymphatic transport of radiocolloid from the injection site and nodal uptake of the radiocolloid are not significant in clinical practice with a highly sensitive, directional GDP.

ACKNOWLEDGMENTS

This article was supported in part by Grant U01CA65121 from the National Cancer Institute. Its contents are solely the responsibility of the authors and do not necessarily represent the official views of the National Cancer Institute.

REFERENCES

1. Cabanas R. An approach for the treatment of penile carcinoma. *Cancer* 1977;39:456–466.
2. Morton DL, Wen D-R, Wong JH, et al. Technical details of intraoperative lymphatic mapping for early stage melanoma. *Arch Surg* 1992;27:392–399.
3. Alex JC, Krag DN. Gamma-probe guided localization of lymph nodes. *Surg Oncol* 1993;2:137–143.
4. Alex JC, Weaver DL, Fairbanks JT, Rankin BS, Krag DN. Gamma probe-guided lymph node localization in malignant melanoma. *Surg Oncol* 1993;2:303–308.
5. Krag DN, Weaver DL, Alex JC, Fairbank JT. Surgical resection and radiolocalization of the sentinel node in breast cancer using a gamma probe. *Surg Oncol* 1993;2:335–340.

6. Krag DN, Meijer SJ, Weaver DL, et al. Minimal-access surgery for staging of malignant melanoma. *Arch Surg* 1995;130:654–658.
7. Albertini JJ, Cruse CW, Rapaport D, et al. Intraoperative radiolymphoscintigraphy improves sentinel node identification in patients with melanoma. *Ann Surg* 1996;223: 217–224.
8. Thompson JF, McCarthy WH, Bosch CMJ. Sentinel node status as an indicator of the presence of metastatic melanoma in regional lymph nodes. *Melanoma Res* 1995;5: 255–260.
9. Reintgen D, Albertini J, Miliotes G, et al. The accurate staging and modern day treatment of malignant melanoma. *Cancer Res Ther Control* 1995;4:183–197.
10. Ross MI, Reintgen D, Balch CM. Selective lymphadenectomy: emerging role for lymphatic mapping and sentinel node biopsy in the management of early stage melanoma. *Semin Surg Oncol* 1993;9:219–223.
11. Larson D, Weinstein M, Goldberg I, et al. Edema of the arm as a function of the extent of axillary surgery in patients with Stage I-II carcinoma of the breast treated with primary radiotherapy. *Int J Radiat Oncol Biol Phys* 1986;12:1575–1582.
12. Kissin MW, Querci della Rovere G, Easton D, Westbury G. Risk of lymphedema after the treatment of breast cancer. *Br J Surg* 1986;73:580–584.
13. Veronesi U, Rilke F, Luini A, et al. Distribution of axillary node metastases by level of invasion. An analysis of 539 cases. *Cancer* 1987;59:682–687.
14. Rosen PP, Lesser ML, Kinne DW, Beattie EJ. Discontinuous or "skip" metastases in breast carcinoma. Analysis of 1228 axillary dissections. *Ann Surg* 1983;197:276–283.
15. Lloyd LR, Waits RK Jr, Schroder D, Hawasli A, Rizzo P, Rizzo J. Axillary dissection for breast carcinoma. The myth of skip metastasis. *Am Surg* 1989;55:381–384.
16. Boova RS, Bonanni R, Rosato FE. Patterns of axillary nodal involvement in breast cancer. Predictability of level one dissection. *Ann Surg* 1982;196:642–644.
17. Toma S, Leonessa F, Romanini A, et al. Predictive value of some clinical and pathological parameters on upper level axillary lymph node involvement in breast cancer. *Anticancer Res* 1991;11:1439–1443.
18. Danforth DN Jr, Findlay PA, McDonald HD, et al. Complete axillary lymph node dissection for stage I–II carcinoma of the breast. *J Clin Oncol* 1986;4:655–662.
19. Giuliano AE, Kirgan DM, Guenther JM, Morton DL. Lymphatic mapping and sentinel lymphadenectomy for breast cancer. *Ann Surg* 1994;220:391–401.
20. Giuliano AE, Dale PS, Turner RR, et al. Improved axillary staging of breast cancer with sentinel lymphadenectomy. *Ann Surg* 1995;222:394–401.
21. Albertini JJ, Lyman GH, Cox C, et al. Lymphatic mapping and sentinel node biopsy in the patients with breast cancer. *JAMA* 1996;276:1818–1822.
22. McCarthy WH, Thompson JF, Uren RF. Commentary. Minimal access surgery for staging of malignant melanoma. *Arch Surg* 1995;130:659–660.
23. Gulec SA, Moffat FL, Carroll RG. The expanding clinical role of intraoperative gamma probes. In: Freeman LM, ed. *Nuclear medicine annual.* Philadelphia: Lippincott-Raven; 1997:209–237.
24. Strand SE, Persson BRR. Quantitative lymphoscintigraphy: basic concepts for optimal uptake of radiocolloids in the parasternal lymph nodes of rabbits. *J Nucl Med* 1979;20:1038–1046.
25. Senofsky GM, Moffat FL, Davis K, et al. Total axillary lymphadenectomy in the management of breast cancer. *Arch Surg* 1991;126:1336–1342.
26. Hung JC, Wiseman GA, Wahner HW, Mullan BP, Taggart TR, Dunn WL. Filtered technetium-99m sulfur colloid evaluated for lymphoscintigraphy. *J Nucl Med* 1995; 36:1895–1901.
27. Alazraki NP, Eshima D, Eshima LA, et al. Lymphoscintigraphy, the sentinel node concept, and the intraoperative gamma probe in melanoma, breast cancer, and other potential cancers. *Semin Nucl Med* 1997;27:55–67.

Carbon-11-Methionine Uptake in Squamous Cell Head and Neck Cancer

Paula Lindholm, Sirkku Leskinen and Maria Lapela
Department of Oncology and Radiotherapy, and Turku PET Centre, University of Turku, Turku, Finland

The purpose of this study was to investigate whether uptake of L-methyl-[^{11}C]-methionine in a tumor is related to the survival of patients with squamous cell cancer of the head and neck. **Methods:** Thirty-nine patients (median age 64 yr) with newly diagnosed squamous cell carcinoma of the head and neck entered a PET study with [^{11}C]-methionine before therapy. Tumor [^{11}C]-methionine uptake was measured as standardized uptake values (SUVs), and the PET results were compared with the clinical follow-up data of the patients. **Results:** All except one of the malignant lesions within the field of view were visible by [^{11}C]-methionine PET. The median tumor SUV was 9.0 (range 4.0–18.8). The median follow-up time for patients still alive is currently 44 mo (range 14–66 mo). No difference in survival was found between patients with tumor SUV equal to or larger than the median and those with tumor SUV smaller than the median. **Conclusion:** Carbon-11-methionine PET imaging is effective in squamous cell head and neck cancer. The amount of [^{11}C]-methionine uptake does not predict the clinical outcome.

Key Words: PET; carbon-11-methionine; head and neck cancer

J Nucl Med 1998; 39:1393–1397

The optimal treatment for most carcinomas of the head and neck is combined radiotherapy and surgery, although an early-stage cancer may be cured with radiotherapy or surgery alone. The tumor stage at diagnosis is of important prognostic value (*1*), but the role of factors related to aggressive clinical behavior and decreased radiocurability of a malignant tumor, e.g., intrinsic radioresistance, still remains unknown. There are also preliminary molecular and immunohistochemical studies showing that increased risk for locoregional relapse (*2*) or aggressive behavior (*3*) of squamous cell carcinoma may be predicted by using biochemical or genetic markers. However, these methods also have limitations. A reliable method for assessing the aggressive clinical behavior of cancer would assist the clinician in planning cancer therapy.

PET imaging with L-methyl-[^{11}C]-methionine is useful in the detection and delineation of both cerebral and extracranial human cancer (*4–7*). Methionine is an essential amino acid, and its transport is regulated by two different transport mechanisms, system A and system L (*8*). High tumor uptake reflects the increased transport of methionine from the blood into cancer cells.

There is some evidence that tumor [^{11}C]-methionine uptake may be related to the biological aggressiveness of cancer, although the results have been contradictory. Carbon-11-methionine accumulation seemed to be associated with the histological grading of brain (*4*), lung (*5*) and uterine cancer (*6*) but not lymphoma (*9*). A correlation was found between high [^{11}C]-methionine uptake and the high percentage of dividing cells in breast cancer (*7*) and in non-small cell lung cancer (*10*), suggesting that [^{11}C]-methionine PET could be used for evaluating the proliferative activity of a tumor.

The tumor stage remains perhaps the only independent prognostic factor in head and neck cancer. However, tumors with a similar clinical stage may respond to radiotherapy at different rates. There exists a great variation in the radioresponse of individual tumors and, because of heterogeneity, also within a single tumor (*11*). A reliable method for predicting the radiocurability of a tumor would be valuable. Proliferative characteristics do not seem to have any significant relationship to the histopathological grading of head and neck cancer (*11*),

Received Aug. 5, 1997; revision accepted Nov. 6, 1997.
For correspondence or reprints contact: Paula Lindholm, MD, Department of Oncology and Radiotherapy, University of Turku, Kiinamyllynkatu 4–8, FIN-20520 Turku, Finland.